

EDINBURGH 98/9
LBNL-41993

Soft-gluon resummation for heavy quark production in hadronic collisions

Nikolaos Kidonakis¹

*Department of Physics and Astronomy
University of Edinburgh
Edinburgh EH9 3JZ, Scotland, UK*

Ramona Vogt

*Nuclear Science Division
Lawrence Berkeley National Laboratory
Berkeley, CA 94720
and
Physics Department
University of California at Davis
Davis, CA 95616*

Abstract

We discuss the heavy quark production cross section near partonic threshold in hadronic collisions, including the resummation of leading and next-to-leading logarithms arising from soft gluon emission. We show how to handle the complications due to the non-universal non-leading logarithms. We give analytical results for the $q\bar{q}$ partonic subprocess and numerical results in the DIS scheme for top quark production at the Fermilab Tevatron where the $q\bar{q}$ channel dominates.

PACS numbers: 12.38.Cy, 13.85.Lg, 14.65.Ha

¹Present address: Department of Physics, Florida State University, Tallahassee, FL 32306-4350

1 Introduction

Heavy quark production has been a topic of intense interest in the last few years, particularly since the discovery of the top quark at the Fermilab Tevatron. The top quark production cross section will be measured with increased precision as Tevatron running continues. It is therefore important to make precise theoretical predictions for the cross section. Calculations of the cross sections for processes such as top quark production are based on the factorization theorems of perturbative quantum chromodynamics (pQCD) [1]. Factorization separates the perturbative, short-distance hard scattering from nonperturbative universal parton distribution functions. The hadronic cross section is then given by the convolution of the perturbatively calculable partonic cross section with the experimentally determined parton densities. Complete calculations of heavy quark production have been carried out up to next-to-leading order (NLO) in the strong coupling constant α_s [2] and the NLO corrections were found to be significant. Calculations to higher orders are formidable and full results do not exist beyond NLO. However, near the final-state production threshold, $z \equiv Q^2/s = 1$, where Q is the invariant mass of the heavy quark pair and s is the square of the center-of-mass energy of the partonic collision, there are large logarithms at each order in the perturbative expansion originating from soft gluon emission which can be resummed to all orders in pQCD. At n th order in perturbative QCD one encounters terms as singular as $(-\alpha_s^n/n!)[\ln^{2n-1}((1-z)^{-1})/(1-z)]_+$, which, when folded with parton distributions, give large and positive corrections [3]. These Sudakov logarithms, arising from the incomplete cancelation between real and virtual corrections near threshold where the energy of the radiated gluon approaches zero, increase the NLO cross section.

Resummation is a result of factorization [4] and is most easily derived in terms of moments of the cross section with respect to the variable $\tau = Q^2/S$, where S is the center-of-mass energy of the incoming hadrons. In moment space the hadronic cross section becomes the product of moments of the parton distributions and the partonic cross section. The physical resummed cross section is obtained upon inversion of the exponentiated moments back to momentum space.

The leading logarithms for heavy quark production arise from soft gluon emission from the quarks and gluons in the incoming hadrons and are therefore universal. They are thus the same as in the Drell-Yan process where

Sudakov resummation was applied some time ago [5, 6]. More recently, leading-log resummed calculations for heavy quark production [7, 8, 9, 10, 11] have been presented, using different methods [7, 10, 11] to invert the moment calculation to momentum space. The differences between the results are at the level of subleading logarithms and are numerically small for top quark production at the Tevatron.

The theoretical framework for the extension of resummation to non-universal next-to-leading logarithms (NLL) for heavy quark hadroproduction has been presented in Refs. [3, 12, 13] in moment space, and has recently been extended to dijet production [14], and single-particle inclusive cross sections [15], including direct photon production [15] and heavy quark electroproduction [16]. The formalism has also been used to study dijet rapidity gaps [17]. Recently a different method for the calculation of the total NLL resummed heavy quark cross section has appeared [18] which agrees with the moment space results in Refs. [3, 12, 13], and has also been applied to direct photon production [19].

Beyond leading logarithms, the color exchange in the hard scattering must be taken into account. In the next section we will present an anomalous dimension matrix, explicitly calculated in Refs. [12, 13], which controls color-sensitive gluon radiation into the final state. Using the results in [12] we have previously calculated the NLL resummed hadronic cross sections for top and bottom quark production at fixed center-of-mass scattering angle [20]. In this paper, we present analytical results for the angle-integrated NLL resummed cross section in the $q\bar{q} \rightarrow Q\bar{Q}$ channel in the DIS scheme. The calculation of $gg \rightarrow Q\bar{Q}$ is similar but more involved and will be discussed in detail elsewhere [21]. In Section 3, we give numerical results for top quark production at the Fermilab Tevatron in the $q\bar{q} \rightarrow t\bar{t}$ channel, which is dominant.

2 Resummation formalism

The resummation of the cross section in moment space is achieved by refactoring the partonic cross section into hard components which describe the truly short-distance hard-scattering, center-of-mass distributions associated with gluons collinear to the incoming partons, and a soft function associated with non-collinear soft gluons. The soft function is a matrix in color space

which satisfies a renormalization group equation whose solution provides a matrix evolution equation, in terms of soft anomalous dimension matrices, that controls threshold logarithms [12]. The relevant anomalous dimension matrices were calculated in Refs. [12, 13] for heavy quark production through light quark annihilation and gluon fusion. At the level of NLL we can diagonalize the matrix equation and calculate the eigenvalues and eigenvectors of the anomalous dimension matrix. The resummed cross section then becomes a sum of exponentials.

As mentioned above, we have previously applied these results to top and bottom quark production near partonic threshold in hadronic collisions at a center-of-mass scattering angle $\theta = 90^\circ$ where the soft anomalous dimension matrix is diagonal [20]. Here we consider the general case of the total angle-integrated cross section where we must diagonalize the matrix and decompose the Born cross section in a particular color tensor basis. The complications are, as we will see below, considerable, even for the $q\bar{q}$ channel.

We now present an analysis of the process $q(p_a) + \bar{q}(p_b) \rightarrow \bar{Q}(p_1) + Q(p_2)$. We define a variable $s_4 = s + t_1 + u_1$ in terms of the Mandelstam invariants $s = (p_a + p_b)^2$, $t_1 = (p_a - p_1)^2 - m^2$, and $u_1 = (p_b - p_1)^2 - m^2$, where m is the heavy quark mass. The value of s_4 depends on the four-momentum k of the radiated gluon and is given near threshold by $s_4 = 2m^2(1 - z) = 2mk^0$. The $q\bar{q}$ resummed partonic cross section is then given by [7, 9, 20]

$$\sigma_{q\bar{q}}^{\text{res}}(s, m^2) = \sum_{i,j=1}^2 \int_{-1}^1 d\cos\theta \left[- \int_{s_{\text{cut}}}^{s-2ms^{1/2}} ds_4 f_{q\bar{q},ij}(s_4, \theta) \frac{d\bar{\sigma}_{q\bar{q},ij}^{(0)}(s, s_4, \theta)}{ds_4} \right], \quad (2.1)$$

where ij is the component in color space of the anomalous dimension matrix, and $d\bar{\sigma}_{q\bar{q},ij}^{(0)}(s, s_4, \theta)/ds_4$ are components of the differential of the Born cross section defined in the same color basis as the anomalous dimension matrix, as explained below.

The function $f_{q\bar{q},ij}$ is given at NLL by the exponential

$$f_{q\bar{q},ij} \equiv \exp[E_{q\bar{q},ij}] = \exp[E_{q\bar{q}} + E_{q\bar{q}}(\lambda_i, \lambda_j)] \quad (2.2)$$

where $\lambda_{i,j}$ are the eigenvalues of the soft anomalous dimension matrix, Γ_S . The universal component, $E_{q\bar{q}}$, is scheme dependent and is known from Drell-Yan production [5, 6]. At NLL in the DIS scheme this universal contribution

is given by [20]

$$E_{q\bar{q}} = \int_{\omega_0}^1 \frac{d\omega'}{\omega'} \left\{ \int_{\omega'^2 \mu^2 / \Lambda^2}^{\omega' \mu^2 / \Lambda^2} \frac{d\xi}{\xi} \left[\frac{2C_F}{\pi} (\alpha_s(\xi) + \frac{K}{2\pi} \alpha_s^2(\xi)) \right] - \frac{3}{2} \frac{C_F}{\pi} \alpha_s \left(\frac{\omega' \mu^2}{\Lambda^2} \right) \right\}, \quad (2.3)$$

where $C_F = (N^2 - 1)/(2N)$, $C_A = N$, $K = C_A(67/18 - \pi^2/6) - 5n_f/9$ [22], Λ is the QCD scale parameter, and $\omega_0 = s_4/(2m^2)$ with N the number of colors and n_f the number of flavors. The NLL color-dependent process-specific contribution to the exponent is [20]

$$E_{q\bar{q}}(\lambda_i, \lambda_j) = - \int_{\omega_0}^1 \frac{d\omega'}{\omega'} \left\{ \lambda_i \left[\alpha_s \left(\frac{\omega'^2 \mu^2}{\Lambda^2} \right), \theta \right] + \lambda_j^* \left[\alpha_s \left(\frac{\omega'^2 \mu^2}{\Lambda^2} \right), \theta \right] \right\}, \quad (2.4)$$

where $i, j = 1, 2$. The s_4 dependence appears only in the argument of the coupling constant. Note that we have introduced a cutoff s_{cut} in the s_4 integration in Eq. (2.1) because, in the exponents, α_s diverges when $\omega'^2 \mu^2 / \Lambda^2 \sim 1$, corresponding to a minimum s_4 of $s_{4,\text{min}} = 2m^2 \Lambda / \mu$. We choose a value of the cutoff consistent with the sum of the first few terms in the perturbative expansion [7, 8, 9, 20], in the range $30s_{4,\text{min}} < s_{\text{cut}} < 40s_{4,\text{min}}$. Note that this corresponds to a cutoff on the soft gluon energy of the order of the decay width of the top, giving a natural boundary of the nonperturbative region (see also the discussion in [10]). The central value in our cutoff range, $s_{\text{cut}} = 35s_{4,\text{min}}$, corresponds to $s_4/(2m^2) = 0.04$ for $m = 175 \text{ GeV}/c^2$ and $\Lambda = 0.2 \text{ GeV}$.

The anomalous dimension matrix is calculated at partonic threshold, $s_4 = 0$, in a color-tensor basis consisting of s -channel singlet and octet exchange,

$$c_1 = c_{\text{singlet}} = \delta_{ab} \delta_{12}, \quad c_2 = c_{\text{octet}} = -\frac{1}{2N} c_1 + \frac{1}{2} \delta_{a2} \delta_{b1}. \quad (2.5)$$

In this basis and in an axial gauge, $A^0 = 0$, the components of Γ_S are [12]

$$\begin{aligned} \Gamma_{11} &= -\frac{\alpha_s}{\pi} C_F (L_\beta + 1 + \pi i), \\ \Gamma_{21} &= \frac{2\alpha_s}{\pi} \ln \left(\frac{u_1}{t_1} \right), \quad \Gamma_{12} = \frac{C_F}{2C_A} \Gamma_{21}, \\ \Gamma_{22} &= \frac{\alpha_s}{\pi} \left\{ C_F \left[4 \ln \left(\frac{u_1}{t_1} \right) - L_\beta - 1 - \pi i \right] \right. \\ &\quad \left. + \frac{C_A}{2} \left[-\ln \left(\frac{u_1^2 m^2 s}{t_1^4} \right) + L_\beta + \pi i \right] \right\}, \end{aligned} \quad (2.6)$$

where

$$L_\beta = \frac{1 - 2m^2/s}{\beta} \left(\ln \frac{1 - \beta}{1 + \beta} + \pi i \right), \quad (2.7)$$

with $\beta = \sqrt{1 - 4m^2/s}$. Note that the matrix Γ_S is diagonal in this singlet-octet basis when $\beta = 0$ and also when $\theta = 90^\circ$ ($u_1 = t_1$) for arbitrary β . It is this property that simplifies the calculation of the cross section at $\theta = 90^\circ$, as shown in Ref. [20].

The eigenvalues λ_i and eigenvectors e_i , with $i = 1, 2$, of the anomalous dimension matrix are given, respectively, by

$$\lambda_{1,2} = \frac{1}{2} \left[\Gamma_{11} + \Gamma_{22} \pm \left((\Gamma_{11} - \Gamma_{22})^2 + 4\Gamma_{12}\Gamma_{21} \right)^{1/2} \right], \quad (2.8)$$

and

$$e_i = \begin{bmatrix} \frac{\Gamma_{12}}{\lambda_i - \Gamma_{11}} \\ 1 \end{bmatrix} \quad (2.9)$$

for each eigenvalue λ_i . Then, if $C = (c_{\text{singlet}}, c_{\text{octet}})$ is the original color basis, the diagonal color basis in which we work is $C' \equiv (c'_1, c'_2) = CR$, where

$$R = [e_1 \ e_2] = \begin{bmatrix} \frac{\Gamma_{12}}{\lambda_1 - \Gamma_{11}} & \frac{\Gamma_{12}}{\lambda_2 - \Gamma_{11}} \\ 1 & 1 \end{bmatrix}, \quad (2.10)$$

and the diagonalized anomalous dimension matrix is

$$\Gamma_S^{\text{diag}} = R^{-1}\Gamma_S R = \begin{bmatrix} \lambda_1 & 0 \\ 0 & \lambda_2 \end{bmatrix}. \quad (2.11)$$

The diagonal color basis is given explicitly by

$$C' \equiv (c'_1, c'_2) = \left(\frac{\Gamma_{12}}{\lambda_1 - \Gamma_{11}} c_{\text{singlet}} + c_{\text{octet}}, \quad \frac{\Gamma_{12}}{\lambda_2 - \Gamma_{11}} c_{\text{singlet}} + c_{\text{octet}} \right), \quad (2.12)$$

or, inversely, $C = C'R^{-1}$, giving for the octet contribution

$$c_{\text{octet}} = \frac{(\lambda_1 - \Gamma_{11})c'_1 - (\lambda_2 - \Gamma_{11})c'_2}{(\lambda_1 - \lambda_2)}. \quad (2.13)$$

Since the Born cross section is pure octet exchange, it is proportional to c_{octet}^2 so that, after squaring Eq. (2.13), the Born cross section is defined in terms

of $|c'_1|^2$, $|c'_2|^2$, and $c'_1 c'_2^*$. Using the relations $c_{\text{octet}}^2 = (N^2 - 1)/4$, $c_{\text{singlet}}^2 = N^2$, and $c_{\text{singlet}} c_{\text{octet}} = 0$, we find

$$|c'_{1,2}|^2 = \frac{N^2 \Gamma_{12}^2}{|\lambda_{1,2} - \Gamma_{11}|^2} + \frac{N^2 - 1}{4} \quad (2.14)$$

and

$$c'_1 c'_2^* = \frac{N^2 \Gamma_{12}^2}{(\lambda_1 - \Gamma_{11})(\lambda_2 - \Gamma_{11})^*} + \frac{N^2 - 1}{4}. \quad (2.15)$$

The resummed partonic cross section can then be written in the diagonal basis as

$$\begin{aligned} \sigma_{q\bar{q}}^{\text{NLL, res}}(s, m^2) = & - \sum_{i,j=1}^2 \int_{-1}^1 d \cos \theta \int_{s_{\text{cut}}}^{s-2ms^{1/2}} ds_4 \frac{1}{|\lambda_1 - \lambda_2|^2} \frac{d\bar{\sigma}_{q\bar{q}}^{(0)}(s, s_4, \theta)}{ds_4} \\ & \times \left[\left(\frac{4N^2}{N^2 - 1} \Gamma_{12}^2 + |\lambda_1 - \Gamma_{11}|^2 \right) e^{E_{q\bar{q},11}} + \left(\frac{4N^2}{N^2 - 1} \Gamma_{12}^2 + |\lambda_2 - \Gamma_{11}|^2 \right) e^{E_{q\bar{q},22}} \right. \\ & \left. - \frac{8N^2}{N^2 - 1} \Gamma_{12}^2 \text{Re} \left(e^{E_{q\bar{q},12}} \right) - 2 \text{Re} \left((\lambda_1 - \Gamma_{11})(\lambda_2 - \Gamma_{11})^* e^{E_{q\bar{q},12}} \right) \right], \quad (2.16) \end{aligned}$$

where

$$\begin{aligned} \frac{d\bar{\sigma}_{q\bar{q}}^{(0)}(s, s_4, \theta)}{ds_4} = & -\pi \alpha_s^2 K_{q\bar{q}} N C_F \frac{1}{4s^4} \frac{s - s_4}{\sqrt{(s - s_4)^2 - 4sm^2}} \\ & \times \left[(3(s - s_4)^2 - 8sm^2)(1 + \cos^2 \theta) + 4sm^2(1 - \cos^2 \theta) \right] \quad (2.17) \end{aligned}$$

is the differential of the Born cross section. The explicit expressions for all the quantities in Eq. (2.16) are long but straightforward to derive. For example, if we define variables r and ϕ by

$$(\Gamma_{11} - \Gamma_{22})^2 + 4\Gamma_{12}\Gamma_{21} = \frac{\alpha_s^2}{\pi^2} r e^{i\phi}, \quad (2.18)$$

we can write the eigenvalues as

$$\lambda_{1,2} = \frac{1}{2} \left[\Gamma_{11} + \Gamma_{22} \pm \frac{\alpha_s}{\pi} r^{1/2} e^{i\phi/2} \right]. \quad (2.19)$$

Then, we find for the exponentials

$$e^{E_{q\bar{q},11(22)}} = \exp \left\{ E_{q\bar{q}} - \int_{\omega_0}^1 \frac{d\omega'}{\omega'} [\text{Re}\Gamma_{11} + \text{Re}\Gamma_{22} \pm \frac{\alpha_s(\omega'^2 \mu^2 / \Lambda^2)}{\pi} r^{1/2} \cos\left(\frac{\phi}{2}\right)] \right\}, \quad (2.20)$$

where the $+(-)$ sign for the last term is for $E_{q\bar{q},11}(E_{q\bar{q},22})$, and

$$\begin{aligned} \text{Re}(e^{E_{q\bar{q},12}}) &= \exp \left\{ E_{q\bar{q}} - \int_{\omega_0}^1 \frac{d\omega'}{\omega'} [\text{Re}\Gamma_{11} + \text{Re}\Gamma_{22}] \right\} \\ &\times \cos \left[- \int_{\omega_0}^1 \frac{d\omega'}{\omega'} \frac{\alpha_s(\omega'^2 \mu^2 / \Lambda^2)}{\pi} r^{1/2} \sin\left(\frac{\phi}{2}\right) \right]. \end{aligned} \quad (2.21)$$

Note that $\text{Im}(e^{E_{q\bar{q},12}})$ is the same as $\text{Re}(e^{E_{q\bar{q},12}})$ above but with the cosine replaced by the sine of the terms in the last square brackets of Eq. (2.21).

3 Numerical results

In this section we present some numerical results for the exponents and the resummed partonic and hadronic top quark production cross sections.

In Fig. 1, the exponents in the resummed cross section, $E_{q\bar{q},11}$ and $E_{q\bar{q},22}$, Eqs. (2.2) and (2.20), along with the universal contribution, $E_{q\bar{q}}$, Eq. (2.3), are given as functions of $s_4/(2m^2)$ in the DIS scheme with $m = 175 \text{ GeV}/c^2$, $\sqrt{s} = 351 \text{ GeV}$, and $\Lambda_5 = 0.202 \text{ GeV}$ to be consistent with the CTEQ 4D parton densities [23, 24]. Note that the absolute value of $E_{q\bar{q},11}$ is given. The color-dependent exponents are considerably larger than $E_{q\bar{q},22}$ at fixed angle, as shown in Fig. 1(a) of the first reference of [20].

In Fig. 2, the partonic top quark cross section, Eq. (2.16), is presented as a function of $\eta = s/(4m^2) - 1$. We show the NLO exact and approximate results as well as the NLL resummed result (with $s_{\text{cut}} = 35s_{4,\text{min}}$). The NLO approximate cross section is the one-loop expansion of our NLL resummed cross section. The lower limit of the η range of the NLL resummed partonic cross section depends on the value of s_{cut} . No cutoff is applied to the NLO approximate results. As shown in [12, 13], the one-loop expansion of the resummed cross section agrees analytically near threshold with the NLO

approximate results in [25], and, as is evident from Fig. 2, is an excellent approximation of the exact NLO cross section in the threshold region (see also Fig. 7 in [25]). We note that the largest contribution to the hadronic cross section comes from the region $0.1 < \eta < 1$ [9, 13].

The NLL resummed hadronic cross section is given by the convolution of parton distributions $\phi_{i/h}$, for parton i in hadron h , with the partonic cross section

$$\sigma_{q\bar{q},\text{had}}^{\text{NLL,res}}(S, m^2) = \sum_{q=u}^b \int_{\tau_0}^1 d\tau \int_{\tau}^1 \frac{dx}{x} \phi_{q/h_1}(x, \mu^2) \phi_{\bar{q}/h_2}\left(\frac{\tau}{x}, \mu^2\right) \sigma_{q\bar{q}}^{\text{NLL,res}}(\tau S, m^2), \quad (3.1)$$

where $\sigma_{q\bar{q}}^{\text{NLL,res}}(\tau S, m^2)$ is defined in Eq. (2.16) and $\tau_0 = (m + \sqrt{m^2 + s_{\text{cut}}})^2 / S$.

Our numerical results for the $t\bar{t}$ production cross section at the Fermilab Tevatron with $\sqrt{S} = 1.8$ TeV are shown in Figs. 3 and 4 as functions of the top quark mass. We use the CTEQ 4D DIS parton densities [23, 24]. Since the parton densities are only available at fixed order, the application to a resummed cross section introduces some uncertainty. The NLO exact cross sections, including the factorization scale dependence, are shown in Fig. 3 along with the NLO approximate cross section, calculated with $s_{\text{cut}} = 0$ and $\mu^2 = m^2$. Again we note the excellent agreement between the NLO exact and approximate cross sections.

The NLL resummed cross section, including the scale dependence, is shown in Fig. 4. The scale dependence is significantly reduced relative to the NLO cross section. Note that implicit in the change of scale is a change of cutoff through the definition of $s_{4,\text{min}}$. To match our results to the exact NLO cross section we define the NLL improved cross section

$$\sigma_{q\bar{q},\text{had}}^{\text{imp}} = \sigma_{q\bar{q},\text{had}}^{\text{NLL,res}} - \sigma_{q\bar{q},\text{had}}^{\text{NLO,approx}} + \sigma_{q\bar{q},\text{had}}^{\text{NLO,exact}}. \quad (3.2)$$

In Fig. 4 the hadronic improved cross section is shown for $\mu^2 = m^2$ along with the variation with s_{cut} . Note that the improved cross section is calculated with the same cut applied to the NLO approximate and the NLL resummed cross sections. This cut reduces the approximate cross section relative to the exact one. The variation of the improved cross section is small over the range $30s_{4,\text{min}} < s_{\text{cut}} < 40s_{4,\text{min}}$.

4 Conclusions

We have given explicit results for the resummed heavy quark production cross section to next-to-leading logarithmic level. We have presented numerical results for the dominant channel, $q\bar{q}$, in the DIS scheme, for $t\bar{t}$ production at the Tevatron. At $m = 175 \text{ GeV}/c^2$ and $\sqrt{S} = 1.8 \text{ TeV}$, the value of the improved cross section for $q\bar{q} \rightarrow t\bar{t}$ with $s_{\text{cut}}/(2m^2) = 0.04$ is $5.7 < \sigma_{q\bar{q},\text{had}}^{\text{imp}} < 6.1 \text{ pb}$ for $m/2 < \mu < 2m$, with a central value of 6.0 pb compared to a NLO cross section of 4.5 pb at $\mu = m$. At the upgraded Tevatron with $\sqrt{S} = 2 \text{ TeV}$, the corresponding range is $7.4 < \sigma_{q\bar{q},\text{had}}^{\text{imp}} < 7.9 \text{ pb}$, with a central value of 7.8 pb compared to a NLO cross section of 5.9 pb at $\mu = m$. We find that the corrections relative to NLO are larger for larger scales. The gg channel is more complicated and a complete analysis will be given elsewhere [21]. Adding the gg contribution we predict a total cross section of 7 pb at $\sqrt{S} = 1.8 \text{ TeV}$, in good agreement with experimental values from CDF, $\sigma_{t\bar{t}} = 7.6_{-1.5}^{+1.8} \text{ pb}$ [26], and D0, $\sigma_{t\bar{t}} = 5.5 \pm 1.8 \text{ pb}$ [27]. Gluon fusion is more important for b -quark production at HERA-B where threshold resummation is also of importance [9]. Our formalism can also be naturally extended to heavy quark inclusive differential distributions in transverse momentum and rapidity [8].

Acknowledgements

The work of N.K. was supported by the PPARC under grant GR/K54601. The work of R.V. was supported in part by the Director, Office of Energy Research, Division of Nuclear Physics of the Office of High Energy and Nuclear Physics of the U. S. Department of Energy under Contract Number DE-AC03-76SF0098. We wish to thank Eric Laenen, Sven Moch, Gianluca Oderda, Jack Smith, and George Sterman for many helpful conversations.

References

- [1] J.C. Collins, D.E. Soper, and G. Sterman, in *Perturbative Quantum Chromodynamics*, ed. A. H. Mueller (World Scientific, Singapore, 1989), p. 1.

- [2] P. Nason, S. Dawson, and R.K. Ellis, Nucl. Phys. **B303**, 607 (1988); W. Beenakker, H. Kuijf, W.L. van Neerven, and J. Smith Phys. Rev. D **40**, 54 (1989); W. Beenakker, W.L. van Neerven, R. Meng, G.A. Schuler, and J. Smith, Nucl. Phys. **B351**, 507 (1991).
- [3] N. Kidonakis and G. Sterman, in *Les Rencontres de Physique de la Vallée d'Aoste, Results and Perspectives in Particle Physics*, ed. M. Greco (INFN-Frascati SIS-Ufficio Pubblicazioni, Italy, 1996), p. 333, hep-ph/9607222.
- [4] H. Contopanagos, E. Laenen, and G. Sterman, Nucl. Phys. **B484**, 303 (1997).
- [5] G. Sterman, Nucl. Phys. **B281**, 310 (1987).
- [6] S. Catani and L. Trentadue, Nucl. Phys. **B327**, 323 (1989); **B353**, 183 (1991).
- [7] E. Laenen, J. Smith, and W.L. van Neerven, Nucl. Phys. **B369**, 543 (1992); Phys. Lett. B **321**, 254 (1994).
- [8] N. Kidonakis and J. Smith, Phys. Rev. D **51**, 6092 (1995).
- [9] N. Kidonakis and J. Smith, Mod. Phys. Lett. A **11**, 587 (1996); hep-ph/9506253; J. Smith and R. Vogt, Z. Phys. C **75**, 271 (1997).
- [10] E.L. Berger and H. Contopanagos, Phys. Lett. B **361**, 115 (1995); Phys. Rev. D **54**, 3085 (1996); *ibid.* D **57**, 253 (1998).
- [11] S. Catani, M.L. Mangano, P. Nason, and L. Trentadue, Nucl. Phys. **B478**, 273 (1996); Phys. Lett. B **378**, 329 (1996).
- [12] N. Kidonakis and G. Sterman, Phys. Lett. B **387**, 867 (1996); Nucl. Phys. **B505**, 321 (1997); in proceedings of *DIS 97*, ed. J. Repond and D. Krakauer (AIP Conf. Proc. No. 407, Woodbury, NY, 1997), p. 1035, hep-ph/9708353.
- [13] N. Kidonakis, Ph.D. Thesis, 1996, hep-ph/9606474.

- [14] N. Kidonakis, G. Oderda, and G. Sterman, Nucl. Phys. **B525**, 299 (1998); hep-ph/9803241, to appear in Nucl. Phys. **B**; talk presented at *DIS 98*, Brussels, April 4-8, 1998, hep-ph/9805279.
- [15] E. Laenen, G. Oderda, and G. Sterman, hep-ph/9806467.
- [16] E. Laenen and S. Moch, hep-ph/9809550; S. Moch, talk presented at *DIS 98*, Brussels, April 4-8, 1998, hep-ph/9805370.
- [17] G. Oderda and G. Sterman, Phys. Rev. Lett. **81**, 3591 (1998); G. Oderda, talk presented at *QCD 98*, Montpellier, July 2-8, 1998, hep-ph/9808384.
- [18] R. Bonciani, S. Catani, M.L. Mangano, and P. Nason, Nucl. Phys. **B529**, 424 (1998).
- [19] S. Catani, M.L. Mangano, and P. Nason, J. High Energy Phys. **9807**, 024 (1998).
- [20] N. Kidonakis, J. Smith, and R. Vogt, Phys. Rev. D **56**, 1553 (1997); N. Kidonakis, in *QCD 97*, Nucl. Phys. (Proc. Suppl.) **B64**, 402 (1998).
- [21] N. Kidonakis and R. Vogt, in preparation.
- [22] J. Kodaira and L. Trentadue, Phys. Lett. B **112**, 66 (1982).
- [23] H.L. Lai, J. Huston, S. Kuhlmann, F. Olness, J. Owens, D. Soper, W.K. Tung, and H. Weerts, Phys. Rev. D **55**, 1280 (1997).
- [24] H. Plathow-Besch, ‘PDFLIB: Nucleon, Pion and Photon Parton Density Functions and α_s Calculations’, Users’s Manual - Version 7.09, W5051 PDFLIB, 1997.07.02, CERN-PPE.
- [25] R. Meng, G.A. Schuler, J. Smith, and W.L. van Neerven, Nucl. Phys. **B339**, 325 (1990).
- [26] F. Abe *et al.* (CDF Collab.), Phys. Rev. Lett. **80**, 2773 (1998).
- [27] S. Abachi *et al.* (D0 Collab.), Phys. Rev. Lett. **79**, 1203 (1997).

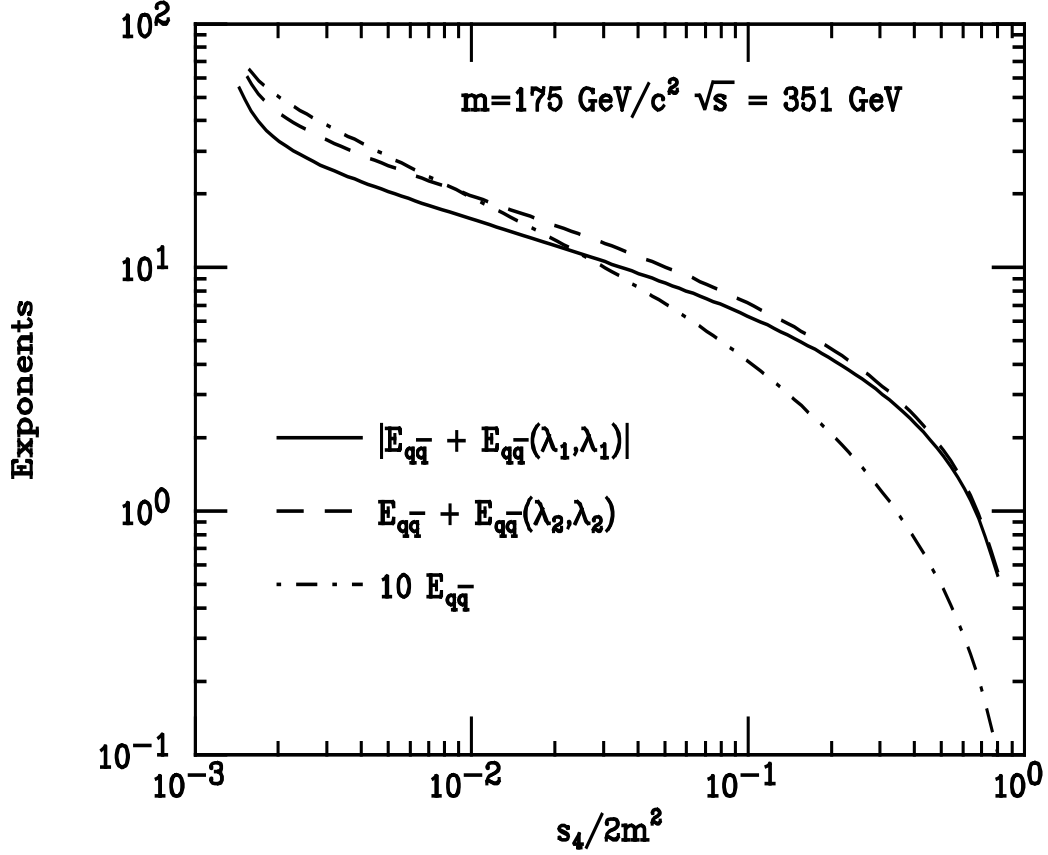


Figure 1: We show the contributions to the $q\bar{q}$ DIS exponents, Eqs. (2.2) and (2.20), in top quark production for $\mu = m = 175 \text{ GeV}/c^2$ and $\sqrt{s} = 351 \text{ GeV}$ as a function of $s_4/(2m^2)$. The solid curve shows the absolute value of $E_{q\bar{q},11}$, the dashed curve, $E_{q\bar{q},22}$. The dot-dashed curve shows $10E_{q\bar{q}}$, Eq. (2.3). The factor of 10 is included to facilitate comparison.

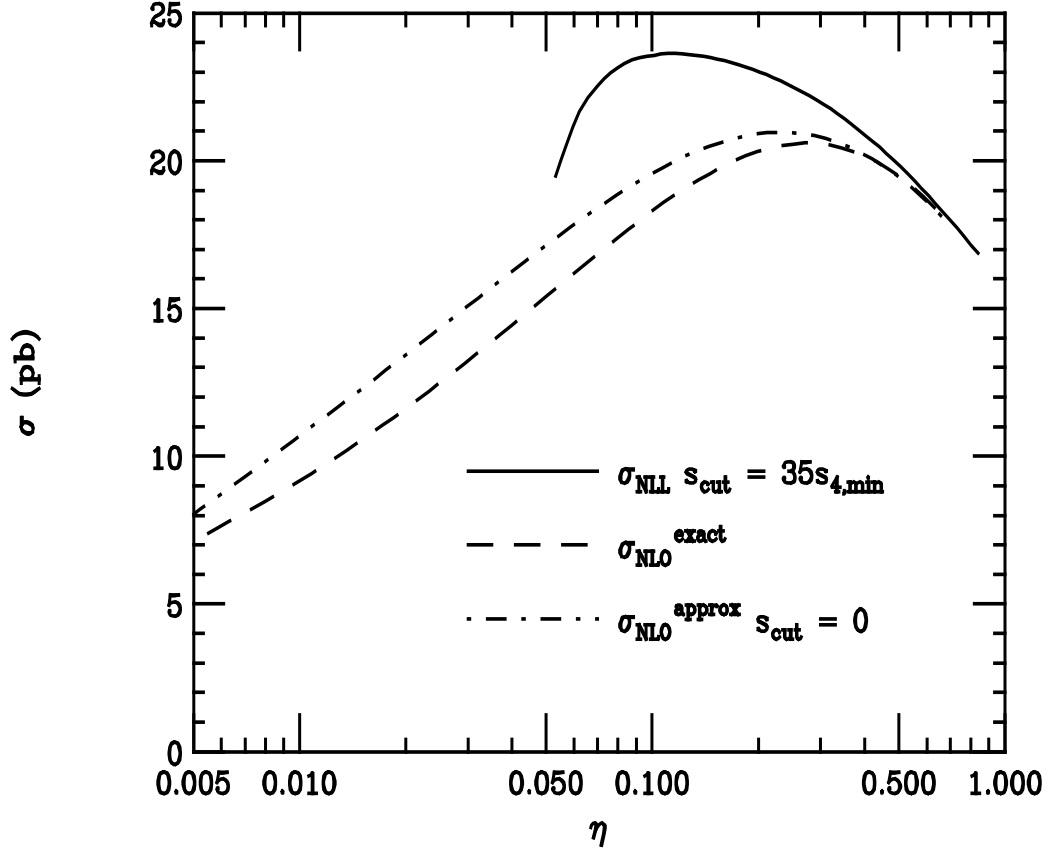


Figure 2: The resummed partonic top quark production cross section, Eq. (2.16), is shown (solid curve) as a function of $\eta = s/(4m^2) - 1$ for the $q\bar{q}$ channel in the DIS scheme and $\mu = m = 175 \text{ GeV}/c^2$ with $s_{\text{cut}} = 35s_{4,\text{min}}$. The NLO exact (dashed) and approximate, with $s_{\text{cut}} = 0$, (dot-dashed) cross sections are also given.

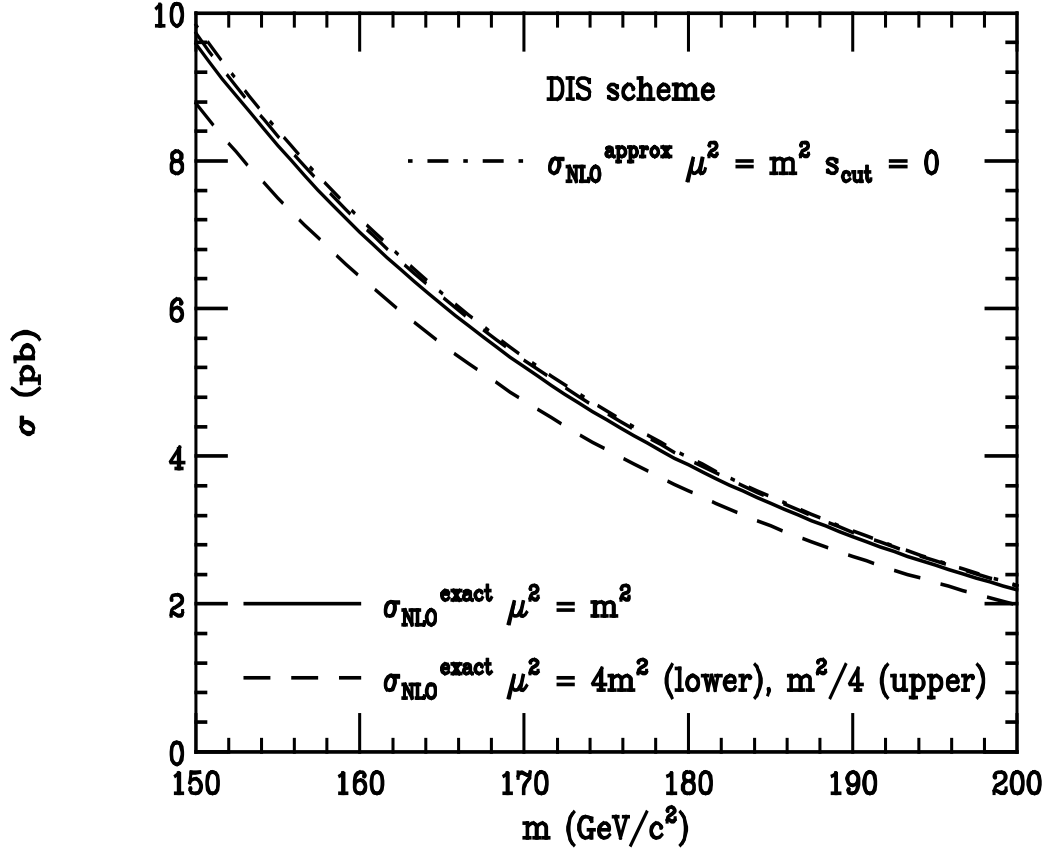


Figure 3: The NLO exact and approximate hadronic $t\bar{t}$ production cross sections in the $q\bar{q}$ channel and the DIS scheme are given as functions of top quark mass for $p\bar{p}$ collisions at the Tevatron energy, $\sqrt{S} = 1.8$ TeV. The NLO exact cross section is given for $\mu^2 = m^2$ (solid curve), $4m^2$ (lower-dashed) and $m^2/4$ (upper-dashed). The NLO approximate cross section with $s_{\text{cut}} = 0$ is shown for $\mu^2 = m^2$ (dot-dashed).

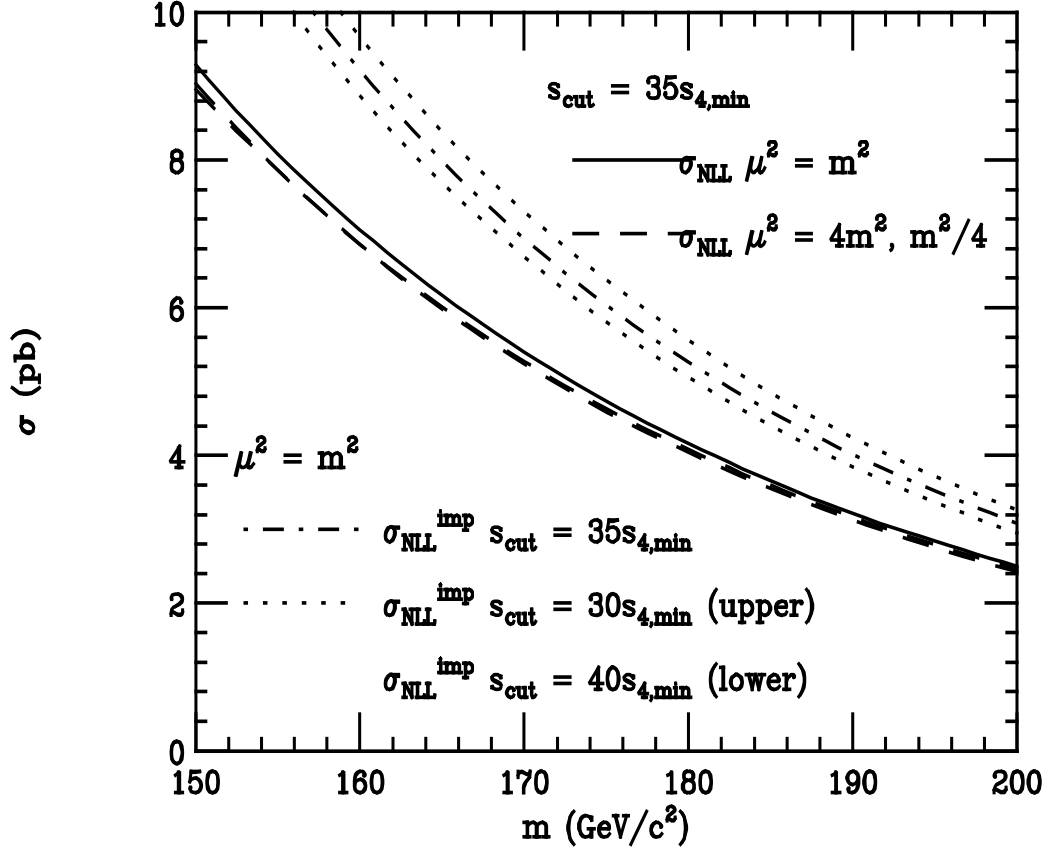


Figure 4: The NLL resummed and improved hadronic $t\bar{t}$ production cross sections in the $q\bar{q}$ channel and the DIS scheme are given as functions of top quark mass for $p\bar{p}$ collisions at the Tevatron energy, $\sqrt{S} = 1.8$ TeV. The NLL resummed cross section, Eq. (3.1), is shown with $s_{\text{cut}} = 35s_{4,\text{min}}$ and $\mu^2 = m^2$ (solid curve), $4m^2$ and $m^2/4$ (both dashed). The NLL improved cross section, Eq. (3.2), is given for $s_{\text{cut}} = 35s_{4,\text{min}}$ (dot-dashed), $30s_{4,\text{min}}$ (upper-dotted) and $40s_{4,\text{min}}$ (lower-dotted).